Lecture No. 6

THE "AVERAGE" TYPHOON

by S. Y. W. Tse

Introduction

Tropical cyclones form one of the many atmospheric circulation systems, which may be conveniently grouped and expressed in terms of various scales of motion after Mason (1970) in Table 1. The term tropical cyclone is used in a generic sense and does not imply any particular intensity. In the western North Pacific and the China Seas area, the most intense are called typhoons, which are equivalent to hurricanes in the Atlantic and the eastern Pacific or "cyclones" in the Indian Ocean. In broad general terms, a mature tropical cyclone is a disturbance consisting of a moist, convective rotating mass of air in which the central part is considerably warmer than the surroundings, up to very high levels. Convective clouds and precipitation elements tend to form curved or spiral bands, which are often organized to exhibit a symmetrical pattern with a circular or elliptical wall cloud around a central region of relatively calm and cloud-free air, known as the eye. The eye diameter usually varies between 10 and 80 n mi, but is often less than 40 n mi. In general, the more intense ones possess smaller eyes. The strongest winds are concentrated in narrow bands around the eye just beyond the edge of the wall cloud.

Since the scales of motion of tropical cyclones overlap those of extratropical depressions to a certain extent, the characteristics of both systems are compared in Table 2. Subtropical cyclones are omitted in this context in order to avoid complications.

The distributions of wind speed and mean pressure profiles and typical thermal structure near the centre in typhoons and comparable extratropical cyclones are markedly different as shown in Figure 1 (Bell 1970). The characteristic dimension and the possible range of the maximum wind speed of tropical cyclones in relation to disturbances of smaller scale are illustrated in Figure 2 (Arakawa et al., 1968). The variation in the size of typhoons (Figure 3) is conspicuous and can be related to differences in synoptic conditions of the environment in which they are embedded and the area of the warm sea underneath. The spectacular difference in size and intensity, which can be represented in terms of minimum central pressure at sea level, from one typhoon to another can be clearly demonstrated in Table 3 and Figure 4 (after Bell, 1970). In addition, the minimum central pressure in typhoons may vary between 990 mb in young ones and 877 mb (Jordan 1959) in the most extreme case.

The magnitude of the fluctuations of the above parameters suggests that available statistics on the average characteristics and structure of typhoons or hurricanes should be viewed as a composite picture in talking about the "average" typhoon.

This lecture purports to deal at some length with the three-dimensional distribution of motion of the "average" typhoon in the composite sense with subsidiary emphasis on the temperature, pressure and moisture fields as could be derived from existing statistics or averages of various typhoons and hurricanes. An attempt is made to discuss their interrelationships. Lastly, the problem of observation and measurement is also dealt with briefly.

Three-dimensional distribution of motion

Composite pictures of the wind circulation around intense tropical cyclones at various levels have been presented by several investigators (Jordan 1952, Hughes 1952, Miller 1958 and Izawa 1964). On average, the typhoon circulation is more extensive than that of the hurricane in both the vertical and horizontal scale; otherwise there is little difference in their circulation patterns (Izawa 1964).

Tangential velocity

The tangential profile of observed winds shows a remarkable asymmetry with the centre of the crescent-shaped maximum wind régime located to the right of the typhoon centre throughout all levels (Figure 5(a)). However, the pattern appears to be approximately symmetrical (except at the surface) after the subtraction of the movement vector from the total wind fields (Figure 6(a)). At the surface, the maximum tangential velocity is about 20 m/sec, but it increases rapidly to about 40 m/sec at 1 km, remains practically constant up to about 9 km and then decreases slowly with height. The vertical profile of the mean tangential velocity obtained by averaging along corresponding rings (circumferential averaging) is shown in Figure 8.

Radial velocity

In the observed wind field, the maximum outflow is located in front of the typhoon centre with peak inflow in the rear (Figure 5(b)). However, the relative positions of maximum outflow and inflow are reversed after subtracting the movement vector of the typhoon centre from the wind fields (Figure 6(b)). This is concordant with the results of Hughes (1952) as depicted by Figure 9. The vertical profile of mean radial velocity (Figure 10) indicates that frictional inflow is restricted to a shallow surface layer, while a deep inflow layer exists near the centre. Outflow occurs near 3 km and around 15 km.

Resultant wind flow

Streamlines (Figure 5(c)) form a spiral pattern only at the surface and are nearly circular above 1 km. The size of the cyclonic circulation decreases gradually with height. Above 12 km, only a very small cyclonic circulation exists near the centre and is surrounded by anticyclonic cells. Relative streamlines are quasi-circular and symmetric above 1 km. The pattern at 15 km is spectacular in demonstrating how cyclonic outflow near the centre leads to widespread anticyclonic outflow into the environment. This is in general agreement with the findings of Jordan (1952) and Fujita (et al., 1967) as shown in Figures 11 and 12.

Vertical velocity, divergence and relative vorticity

As shown in Figure 7(a), upward motion prevails around the core and the area of maximum upcurrent is located to the rear side of the centre. Subsidence occurs at the centre and just outside the regime of ascending motion ahead of the typhoon. The profile of circumferential mean vertical motion (Figure 13) reveals that upcurrent is mainly restricted to a ring of about 4 deg lat. around the eye at the surface, gradually narrowing to 3 deg lat. at about 12 km. The maximum descending motion occurs at the top levels immediately outside the region of strong ascending motion.

The divergence pattern (Figure 7(b)) shows marked asymmetry with maximum divergence in front and maximum convergence in the rear of the typhoon. Thus results obtained by circumferential averaging may not be taken as representative of the mean pattern.

The relative vorticity configuration (Figure 7(c)) also exhibits significant asymmetry. Maximum cyclonic vorticity is found on the right side of the typhoon at all levels. However, the area of cyclonic vorticity diminishes with height and the pattern becomes ill-defined above 15 km. The vertical profile of the mean relative vorticity (Figure 14) shows that maximum cyclonic vorticity occurs near the centre from about 1 km to 9 km.

Pressure and temperature fields

The vertical structure of intense tropical cyclones, particularly hurricanes, has been examined by many investigators (e.g. Palmen, 1948 and Koteswaram, 1967) in terms of temperature and pressure fields. The assumption of axial symmetry gives a good picture of the configuration in general. The model presented by Palmen (1948) is a familiar feature in well-known standard textbooks (e.g. Riehl, 1954) and this is reproduced here as Figure 15. Recently Bell and Tsui (1970) have been compiling statistics about the mean soundings near typhoons. Data extracted from their preliminary analyses were used to construct the profiles of the spatial distributions of pressure and temperature associated with the "average" typhoon in the composite sense under the assumption of axial symmetry as shown in Figure 16, which compares favourably with Palmen's model.

Moisture field

Much remains unknown about the spatial distribution of moisture in typhoons. However, we can infer that the peak moisture concentration should be found in spiral rain bands. Time-lapse radar cine-films reveal that the system of spiral rainbands often rotate anticlockwise around the typhoon centre. This makes collection and collation of moisture data extremely difficult. Gentry (1964) showed that on average, radar rainbands prevail over only about 13 per cent of the areal coverage in the storm's circulation. The percentage coverage could vary considerably in different sectors and from storm to storm (Figure 17). In general, such precipitating clouds are more predominant Equatorward and westward of the centre. Recently, a well-documented case study (Sheets, 1968) shows that the mixing ratios reflected the same general characteristics as the temperatures: "the largest horizontal gradients

occurred near the middle levels, at least within 150 n mi of the storm centre; and the largest maximum anomaly values were found at the middle levels within 150 n mi of the storm centre."

Interrelationships of the distributions of motion, pressure, temperature and moisture

With the aid of Figure 16, which is derived from the basic data just presented, the interrelationships of the distributions of motion, pressure, temperature and moisture in the "average" typhoon may be discussed in terms of the various physical processes responsible for bringing about and maintaining these distributions as follows:

In a conditionally unstable tropical atmosphere over a large warm sea area frictionally forced convergence in the lowest layer can produce a large number of cumuli and cumulonimbi over a wide area. These convective clouds, particularly the tall ones act to transport heat as well as momentum from low levels to the upper troposphere. If the kinetic energy generated by the release of latent heat of condensation can counterbalance frictional "drainage" (dissipation of kinetic energy) and direct transportation of energy to the environment, a steady state can be maintained. As the air particles move spirally inward towards the centre, the effect of centripetal force and other factors prevent penetration beyond a certain minimum radius. Thus air is forced to go upwards with eventual outflow in the upper troposphere. This leads to the formation of the eye wall. As the cyclonic circulation intensifies, particularly around the edge of the eye wall, frictional drag entrains a small amount of the relatively calm air in the eye into the wall cloud at low levels. This induces feeble subsidence in the eye with some dynamic warming. Consequently, marked temperature rise is observed in the central core at all levels and the characteristic temperature distribution is well reflected in the average typhoon, while the isobaric surfaces fall below and rise above (about) 250 mb to maintain hydrostatic equilibrium in the warm core.

A pronounced imbalance in the thermal wind relationship is maintained practically throughout the entire depth of the "average" typhoon circulation. Mass transport to the environment appears to be initiated by cyclonic outflow in the upper troposphere.

Problems of observation and measurement

The instruments used to make observations and measurements of parameters and meteorological elements vary to a great extent in type as well as in response. Furthermore, the properties which may be used to describe the structure of the typhoon or track its movement also fluctuate with time. In addition, different ways of observation may give rise to discordant information which needs reconciliation in operational analysis. In this connexion, the size of the typhoon and its eye may serve as two good examples to illustrate the difficulties which are likely to confront forecasters and analysts.

In practice, the size of the typhoon can be taken as the shortest radius of the outermost closed isobar drawn to the nearest millibar, the size of the cloud mass from satellite pictures excluding the cirrus canopy, or the equivalent radius of the effective area over which spiral rainbands are predominant. However, in all cases, the determination is somewhat subjective.

As regards eye reports, we may have to analyse any combination of the following:

(a) The pressure eye - point of minimum sea-level barometric pressure;

(b) The wind eye - zone of relatively calm air in the typhoon centre;

(c) The radar eye - centre determined by the pattern of rain echoes;

(d) APT eye - apparent clear spot near the centre of the typhoon cloud mass in "Automatic Picture Transmission" satellite photographs;

(e) HRIR eye - apparent clear spot near the centre of the typhoon cloud mass as revealed by the distribution of cloud top temperatures in "High Resolution Infra-red" satellite photographs.

There are inherent inaccuracies in each type of eye report and these reports do not usually agree with one another. Great care must be exercised to reconcile conflicting information or reports. In all cases, we have to rely heavily on intuition and continuity to maintain consistency on an operational basis. However, experience confirms that this exercise is more than rewarding in upkeeping a relatively high standard of proficiency.

Acknowledgments

Grateful thanks are due to Mr. G. J. Bell, J.P., Director of the Royal Observatory for valuable advice and enlightening discussions and to Mr. P. C. Chin, Senior Scientific Officer, for constructive criticisms.

References

Arakawa, H., Watanabe K. and Tsuchiya, K., 1968: A mesometeorological study of a subtropical mesocyclone. Satellite and Meteorology Research Project, Research Paper No. 68, 28 pp.

Bell, G. J., 1970: An introduction to typhoons (manuscript).

Fujita, T., Izawa, T., Watanabe, K. and Imai, I., 1967: A model of typhoons accompanied by inner and other rainbands. Journal of Applied Meteorology, vol. 6, pp. 3-19.

Gentry, R. C., 1964: A study of hurricane rainbands. National Hurricane Research Project, Report No. 69, 85 pp.

Hughes, L. A., 1952: On the low-level wind structure of tropical cyclones. Journal of Meteorology, vol. 9, pp. 422-428.

Izawa, T., 1964: On the mean wind structure of typhoons. Technical Note No. 2, Typhoon Research Laboratory, Meteorological Research Institute, Tokyo, 19 pp.

Jordan, C. L., 1959: Monthly Weather Review, vol. 87, pp. 365.

Jordan, E. S., 1952: An observational study of the upper-wind circulation around tropical storms. Journal of Meteorology, vol. 9, pp. 340-346.

Koteswaram, P., 1967: On the structure of hurricanes in the upper troposphere and lower stratosphere. Monthly Weather Review, vol. 95, pp. 541-564.

Mason, B. J., 1970: Future developments in meteorology: an outlook to the year 2000. Quarterly Journal of the Royal Meteorology Society, vol. 96, pp. 349-368.

Miller, B. I., 1958: On the maximum intensity of hurricanes. Journal of Meteorology, vol. 15, pp. 184-195.

Palmen, E., 1948: On the formation and structure of tropical hurricanes. *Geophysica* (Helsinki), vol. 3, pp. 26-38.

Riehl, H., 1954: Tropical Meteorology, Chapter 11, McGraw-Hill, New York.

Sheets, R. C., 1968: The structure of Hurricane Dora (1964). Technical Memorandum ERLTM-NHRL 83, ESSA Research Laboratories, Florida, 64 pp.

Tsui, K. S., 1970: The vertical temperature and height anomalies of typhoons and hurricanes (manuscript).

TABLE 1

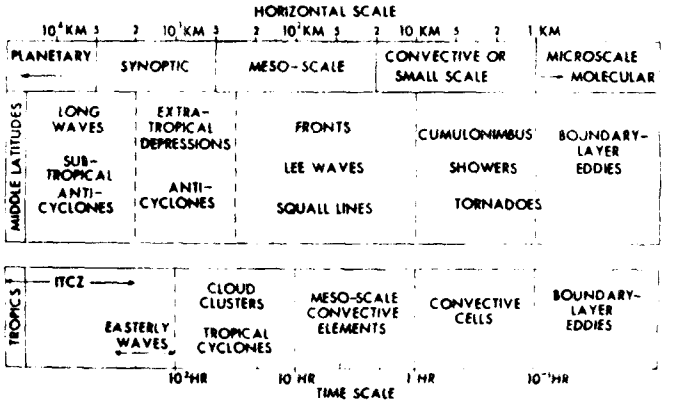

SCALES OF MOTION

(after Mason, 1970)

TABLE 2

Comparison of the characteristics of tropical cyclones and extratropical depressions

Characteristics	Tropical cyclones	Extratropical depressions
Source region	Tropics	Middle latitudes
Horizontal scale (radius)	100–1 000 * km	300–2 000 km
Time scale	10–100 * hr	30–250 hr
Environment	One air mass	Two air masses
Predominant Precipitation	Convective	Non-convective
Frontal system	Absent	Present
Eye	Present	Absent
Circulation	Quasi-symmetric	Non-symmetric
Upper tropospheric thermal structure	Warm core	Warm tongue
Banded structure	Marked	Not marked
Wind régime	Concentrated in narrow bands around eye	Spreading over a wide area
Peak intensity of intense ones	60–200 kt	60–100 kt

* This limit may be exceeded in extreme cases.

TABLE 3

Relative percentage frequency of occurrence of the shortest radius of the outermost isobar (1 mb interval) and of the 1000 mb isobar in tropical cyclones which at some time attained at least severe tropical storm intensity as determined by aircraft reconnaissance

(1958-1968)

Range of radii		All observations		Largest for each tropical cyclone		At the time of minimum pressure	
		1000 mb isobar	Outermost isobar	1000 mb isobar	Outermost isobar	1000 mb isobar	Outermost isobar
deg lat.	km	%	%	%	%	%	%
0.0 - 0.9	0 - 100	15.8	1.4	6.7	0.0	21.5	1.3
1.0 - 1.9	110 - 210	35.9	11.0	28.2	3.1	33.9	18.3
2.0 - 2.9	220 - 320	25.0	23.2	25.1	8.4	24.3	22.8
3.0 - 3.9	330 - 430	13.2	23.0	17.9	11.6	12.4	18.3
4.0 - 4.9	440 - 540	6.8	16.9	12.3	19.6	3.4	16.5
5.0 - 5.9	550 - 660	2.6	11.9	7.2	19.1	2.8	13.4
6.0 - 6.9	670 - 770	0.5	7.0	1.5	14.2	1.7	4.0
7.0 - 7.9	780 - 880	0.1	3.5	0.5	10.2	0.0	3.6
8.0 - 8.9	890 - 990	0.1	1.5	0.5	8.0	0.0	0.9
9.0 - 9.9	1000 - 1100	0.0	0.7	0.0	5.8	0.0	0.9

(after Bell, 1970)

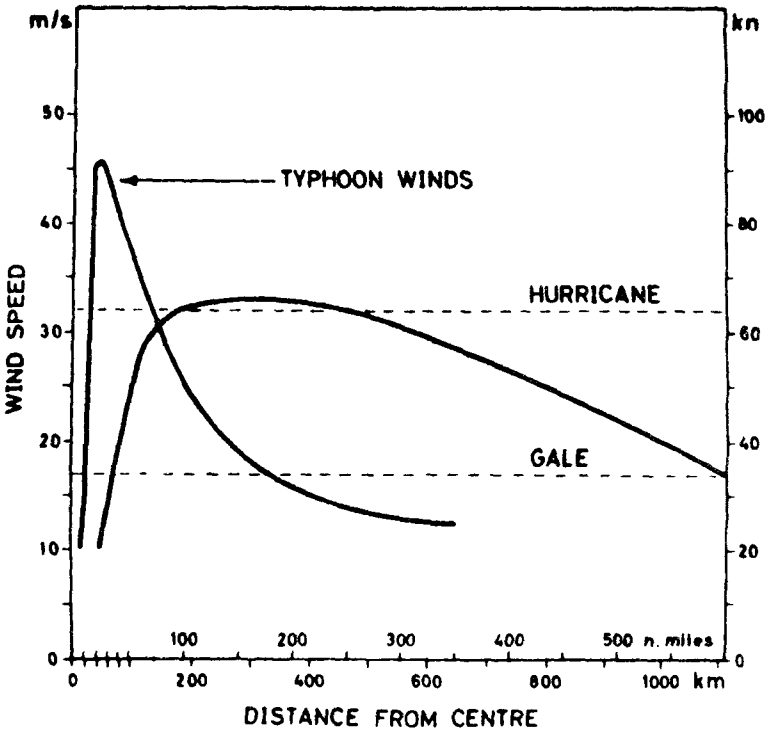

Figure 1(a) - The distribution of wind speed in typhoons and comparable extra-tropical cyclones. The curve for extratropical cyclones was derived from 13 intense Pacific winter storms having central pressures close to 950 mb (after Bell, 1970)

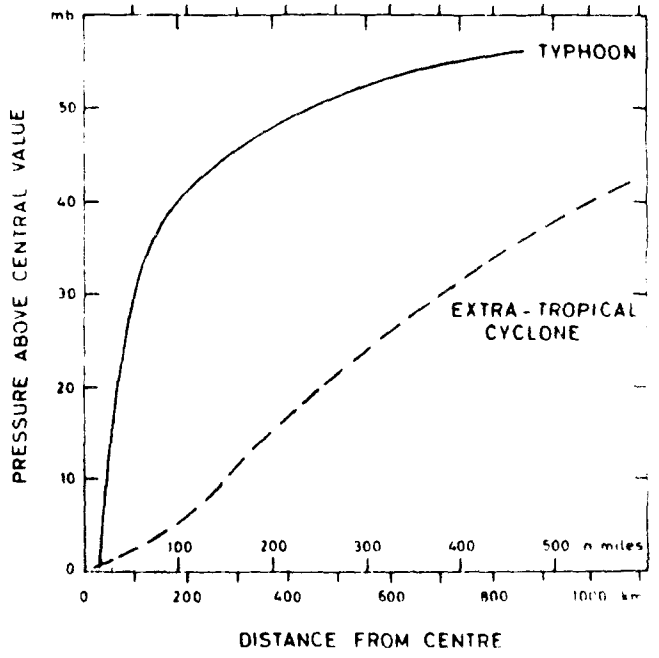

(after Bell, 1970)

Figure 1(b) - Mean pressure profiles from 14 extratropical depressions and 25 typhoons all having minimum central pressures of approximately 950 mb. The pressures in the individual typhoons and extratropical cyclones varied from 937 to 963 mb and 944 to 968 mb respectively

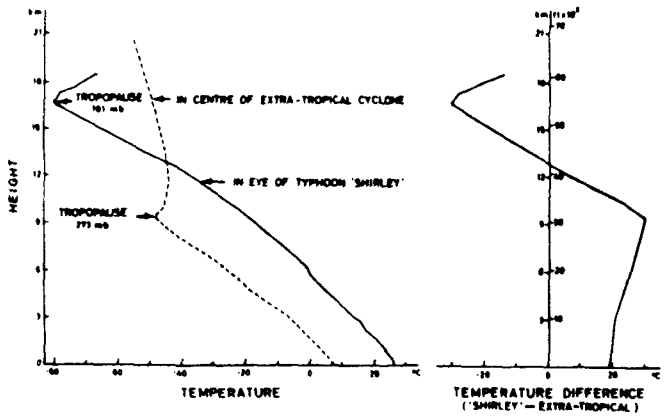

Figure 1(c) - The variation of temperature with height in (1) the eye of typhoon 'Shirley' whilst crossing the Royal Observatory Hong Kong at 1015 GMT on 21 August 1968 and (2) the centre of an extratropical cyclone over Shemyu (lat.52.6 N, long.174.4 E) at 1200 GMT on 10 October 1960. The mean sea-level pressure in 'Shirley' and the extratropical cyclone was 969 and 953 mb respectively

(after Bell, 1970)

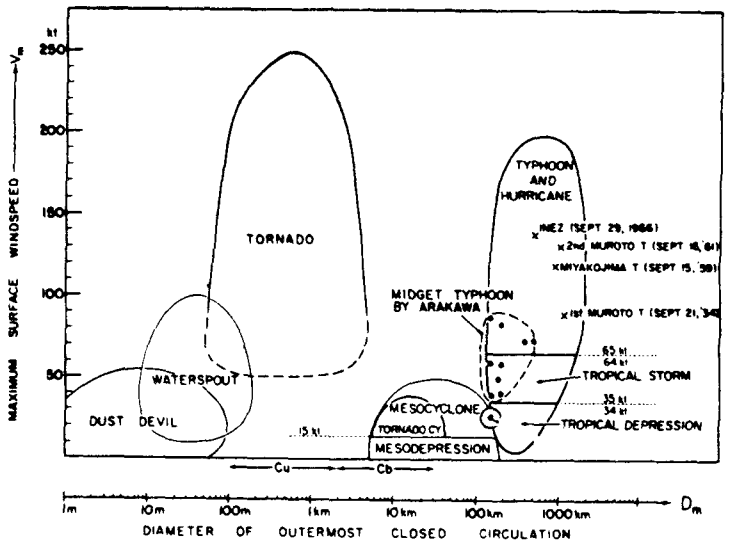

Figure 2 - Characteristic dimension of meteorological disturbances. Their possible range of the maximum wind speed and the circulation diameter is outlined for each disturbance

(after Arakawa et al., 1968)

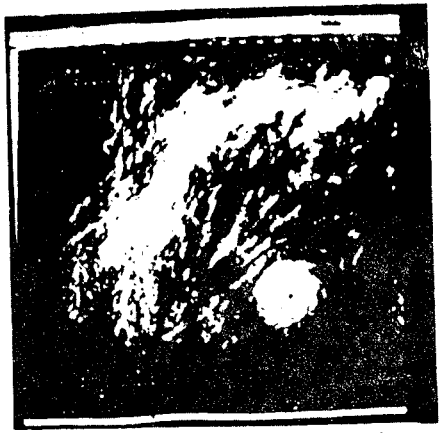

T. ALICE 0050Z 3/9/66

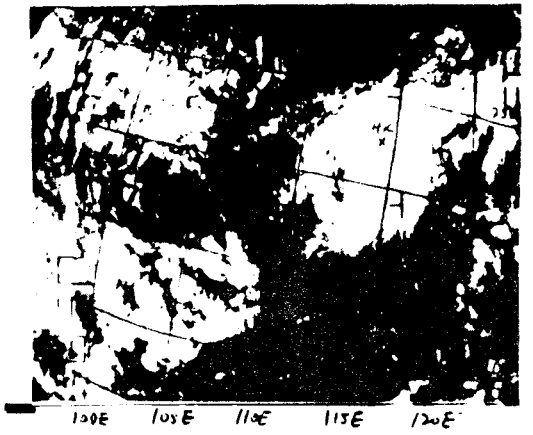

T. IRIS 0746Z 6/10/70

S.T.S. JUDY 0333Z 28/5/66

T. KIT 0001Z 27/6/66

Figure 3(a) - A synopsis of variations in the size of typhoons as revealed by satellite photographs

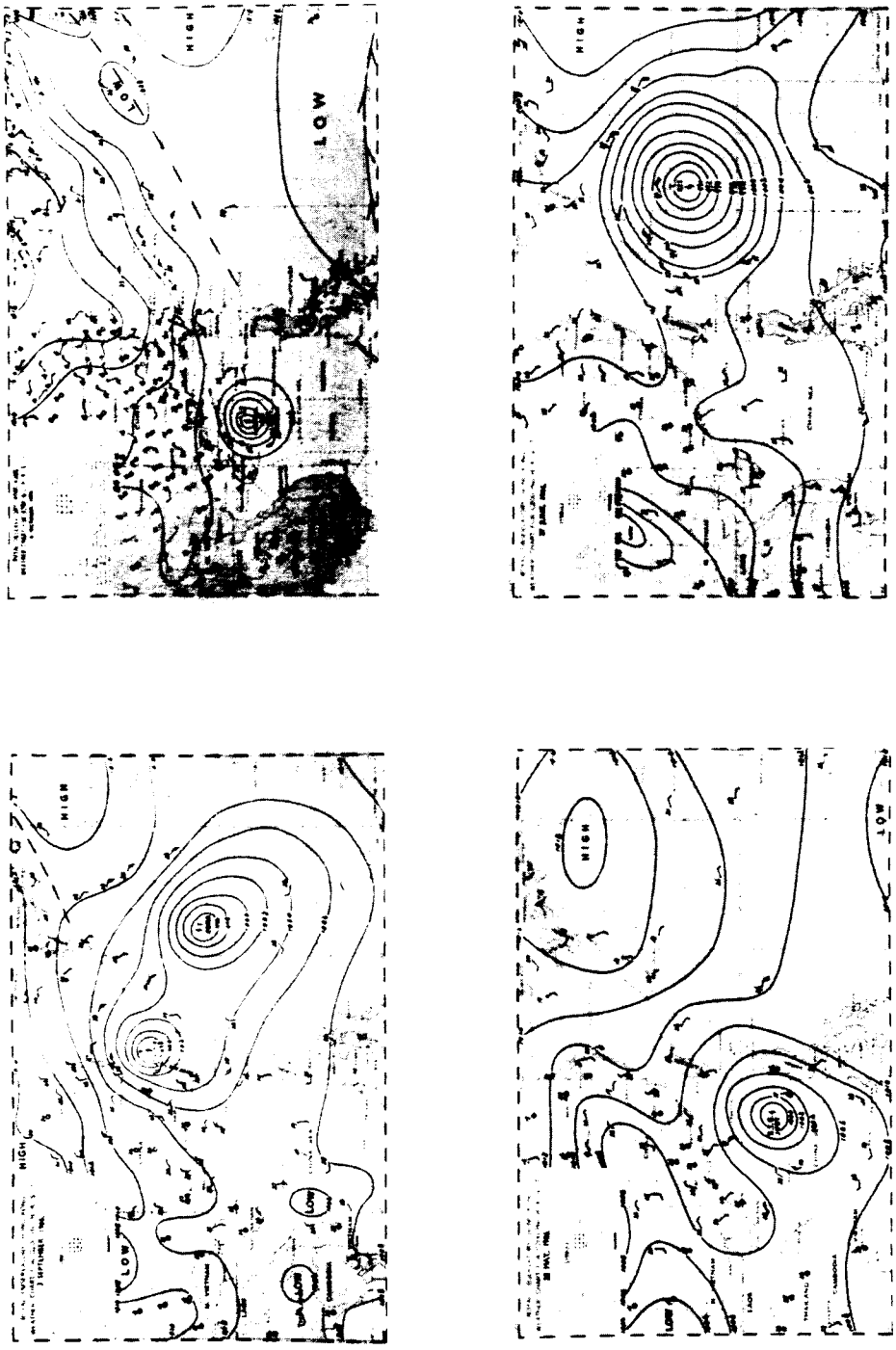

Figure 3(b) - A synopsis of variations in the size of typhoons as depicted by surface weather charts

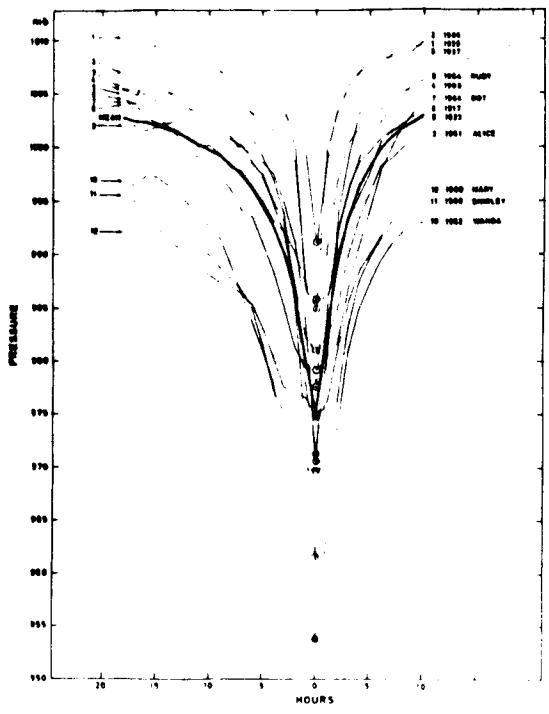

Figure 4(a) - Hourly readings of the barometer at the Royal Observatory Hong Kong before and after the passage of 12 typhoons which caused gales there. The readings have been corrected for the normal diurnal variation of pressure and the curves are centred on the time of the lowest pressure. The heavy curve is the mean of the other twelve

(after Bell, 1970)

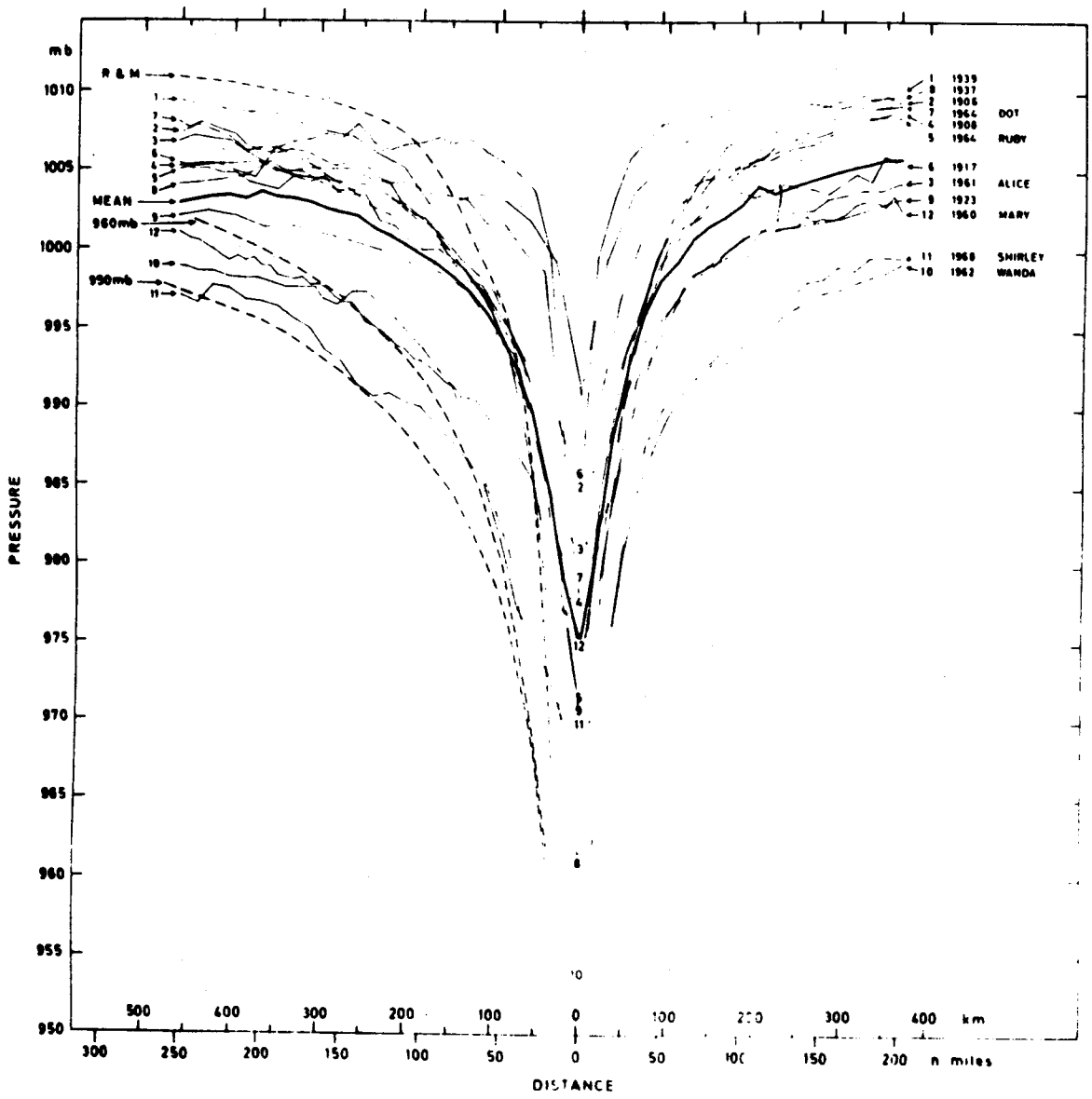

Figure 4(b) – The hourly pressure readings of Figure 4(a) are here plotted against distance from the typhoon centres. The heavy curve is the mean pressure profile. The curve marked R & M refers to the pressure profile in the hurricane (963 mb) proposed by Riehl and Malkus. The curves marked 960 mb and 950 mb are the mean of pressures in 6 and 11 typhoons with central pressure close to the indicated values

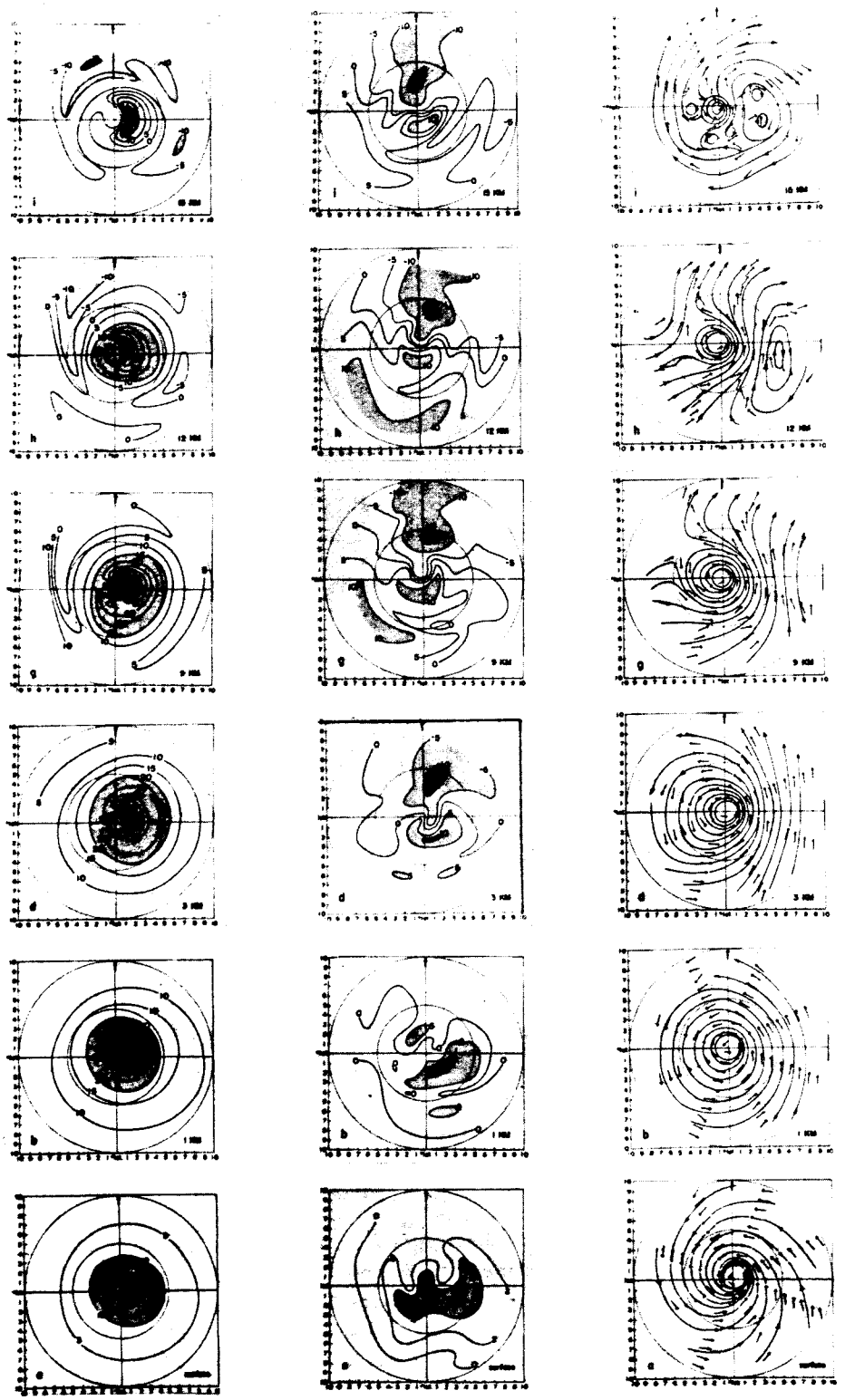

(a) Tangential velocity (b) Radial velocity (c) Streamlines

Figure 5 - Three-dimensional distribution of observed velocity (after Izawa, 1964)

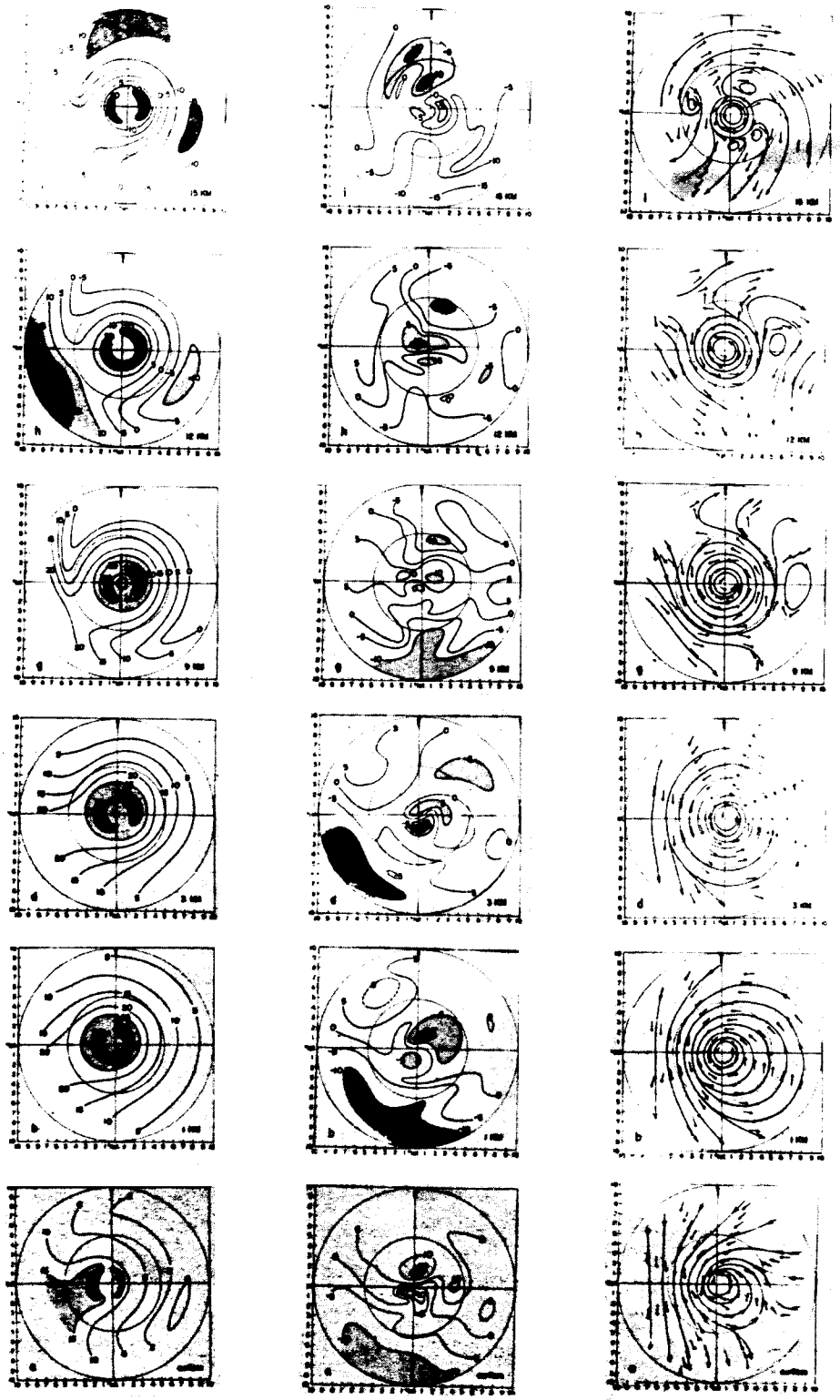

(a) Relative tangential velocity

(b) Relative radial velocity

(c) Relative streamlines

Figure 6 - Three-dimensional distribution of relative velocity (m/sec) (after Izawa, 1964)

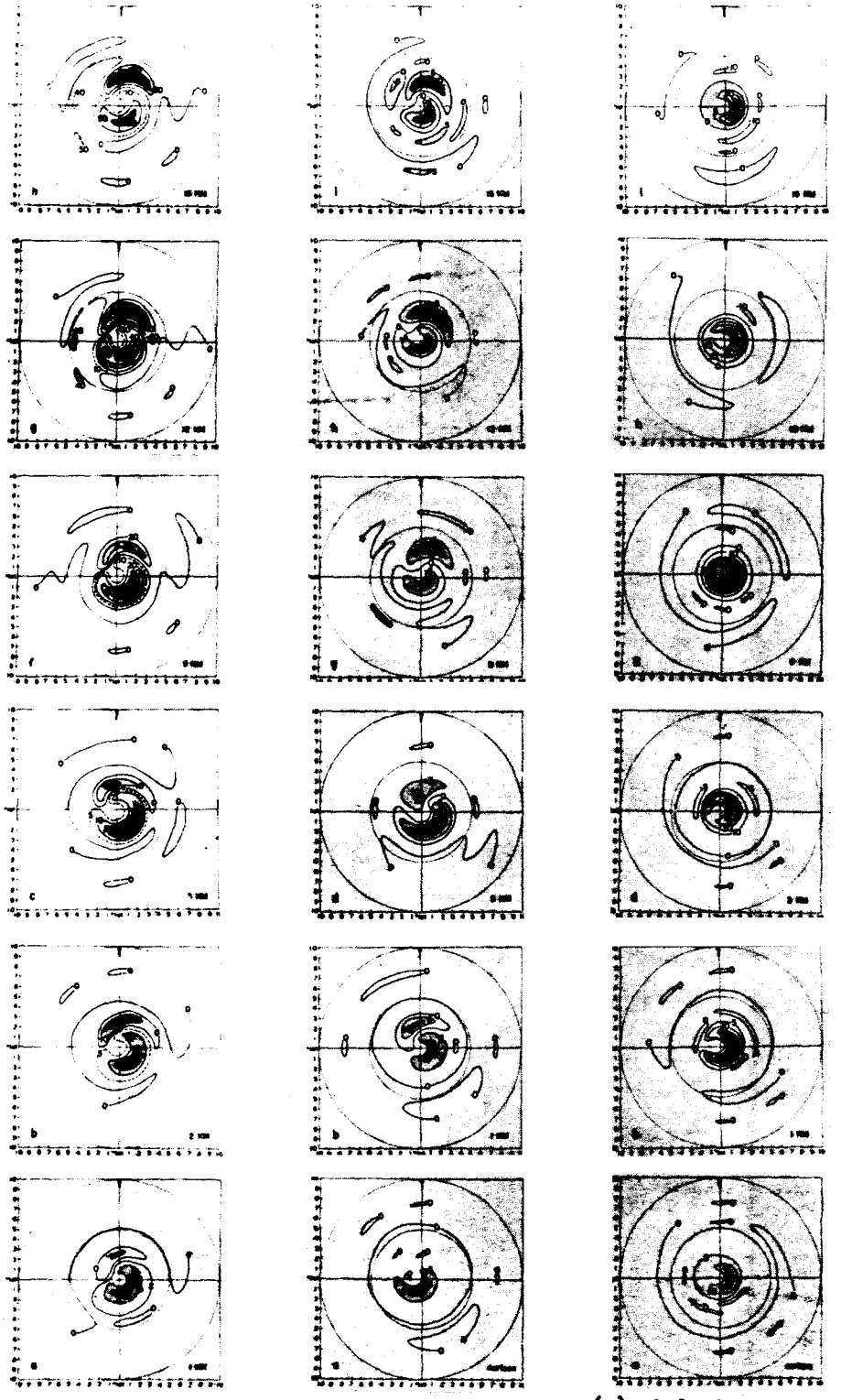

(a) Vertical velocity (cm/sec)

(b) Divergence (10^{-5} sec^{-1})

(c) Relative vorticity (10^{-5} sec^{-1})

Figure 7 - Three-dimensional distribution of vertical velocity, divergence and relative vorticity

(after Izawa, 1964)

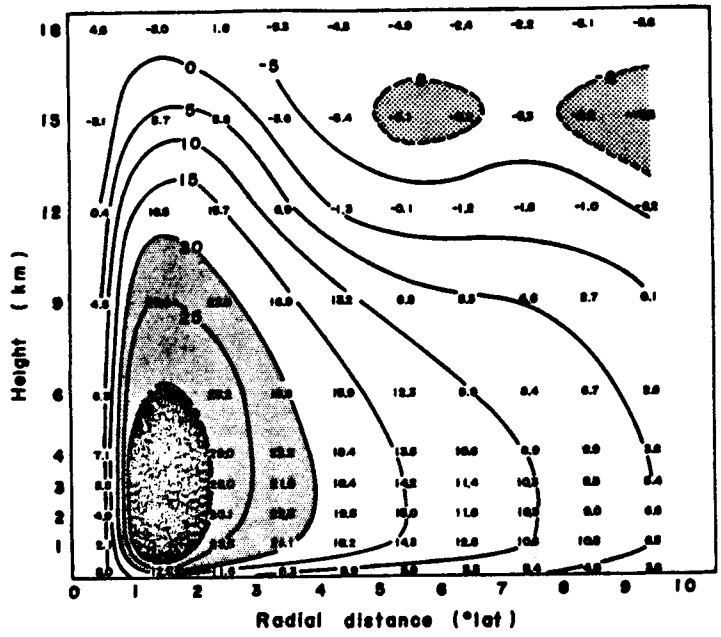

Figure 8 - Vertical cross-section of mean tangential velocity (m/sec). Positive cyclonic

(after Izawa, 1964)

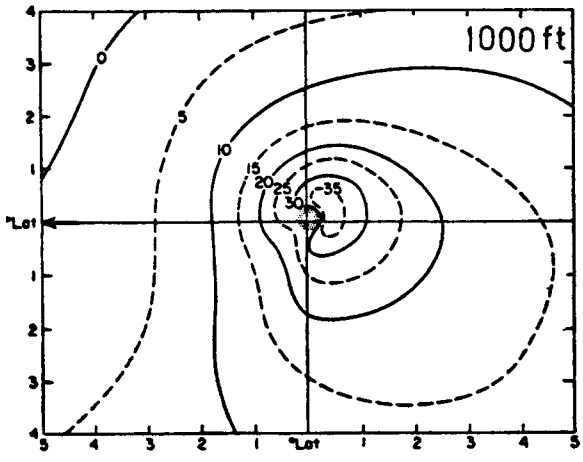

Figure 9(a) - Radial velocity (knots)

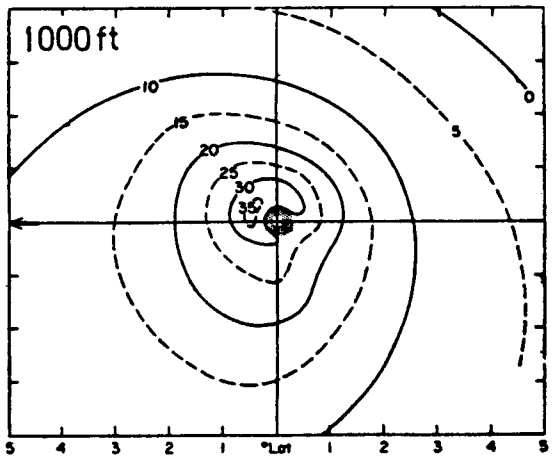

Figure 9(b) - Radial velocity relative to storm (knots)

(after Hughes, 1952)

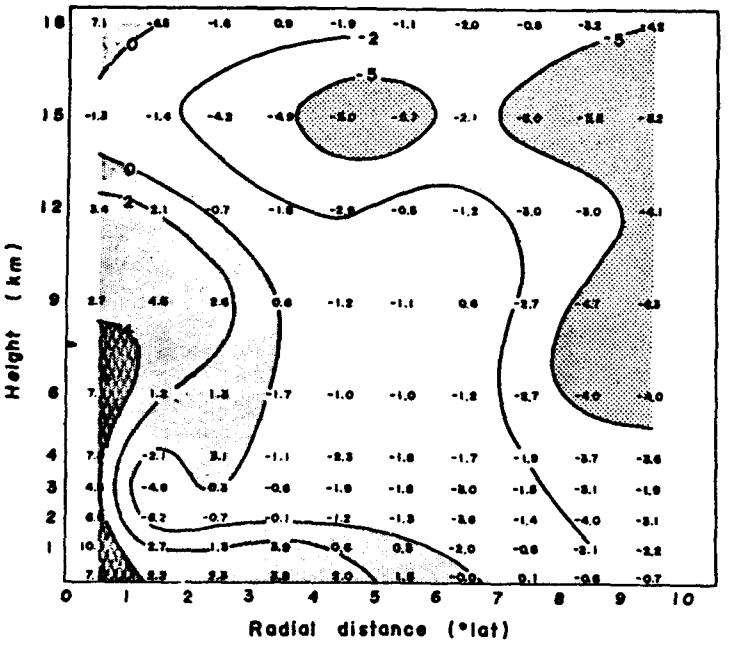

Figure 10 - Vertical cross-section of mean radial velocity (m/sec). Positive for inflow

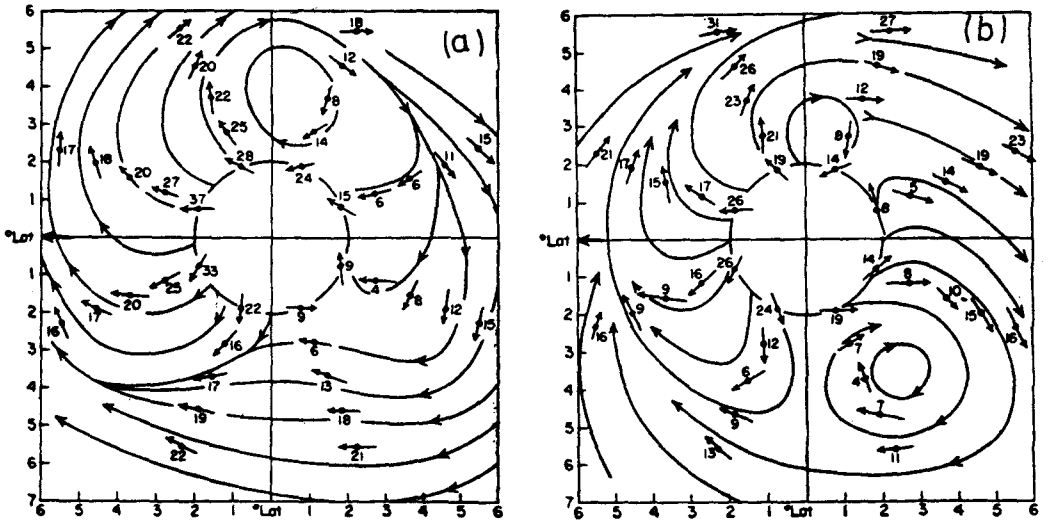

Figure 11 - Total velocity at 45 000 feet (a) and flow relative to moving centre at 45 000 feet (b)

(after Jordan, 1952)

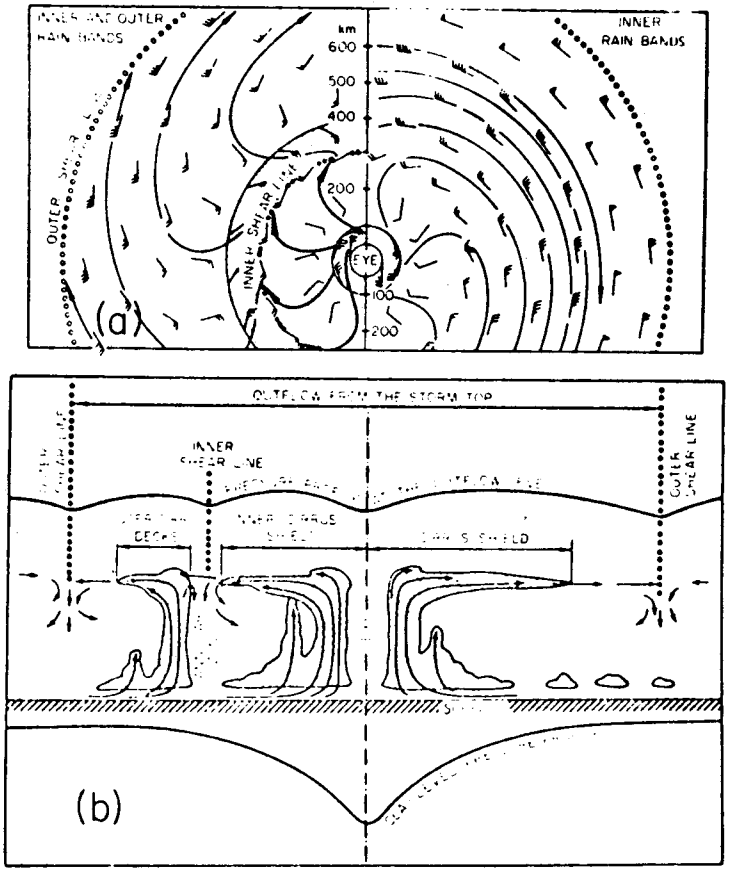

Figure 12 - (a) Two-dimensional distribution of outflow winds for a model typhoon with an inner rain band between 50 and 100 km from the centre (right half). The left half represents a model with an outer rain band in addition to the inner. (b) Vertical section corresponding to these two models. Note that the radial dimensions do not correspond in the two figures

(after Fujita et al., 1967)

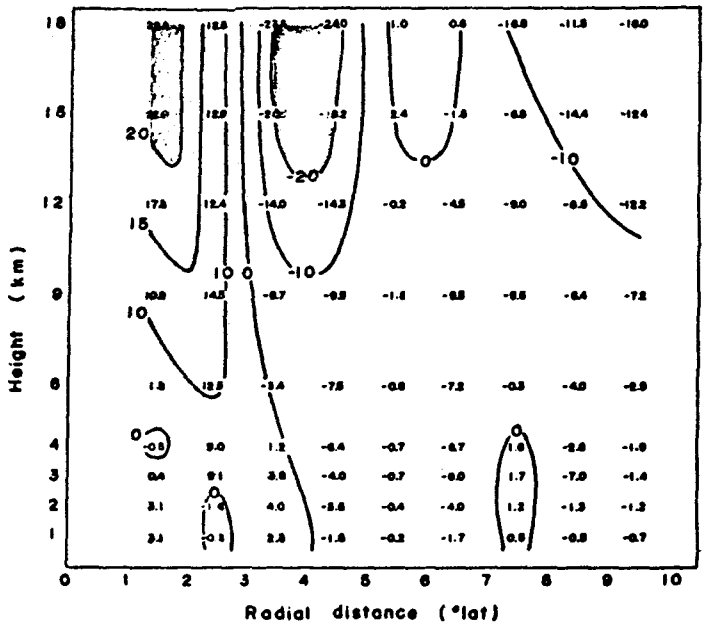

Figure 13 - Vertical cross-section of the mean vertical velocity in (cm/sec). Positive upward

(after Izawa, 1964)

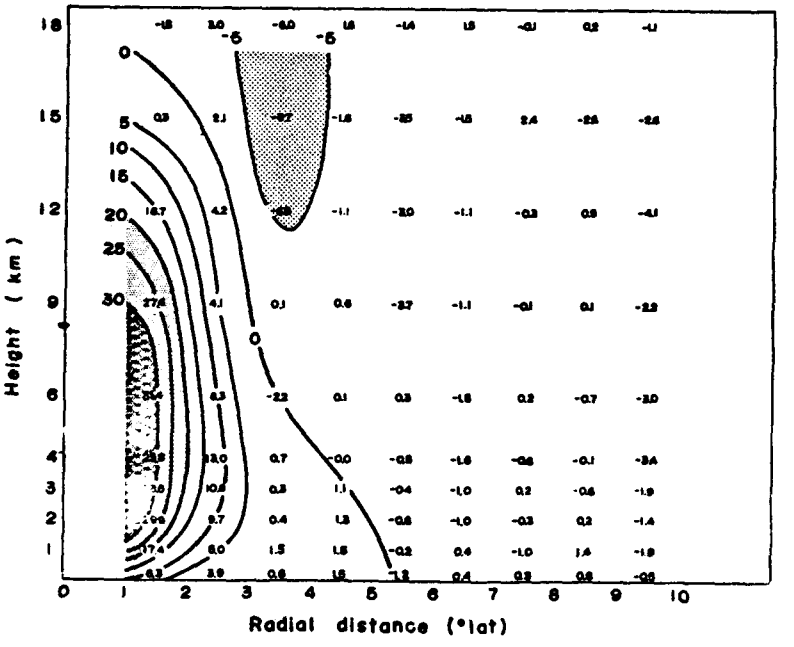

Figure 14 - Vertical cross-section of the main relative vorticity (10^{-5} sec^{-1})
(after Izawa, 1964)

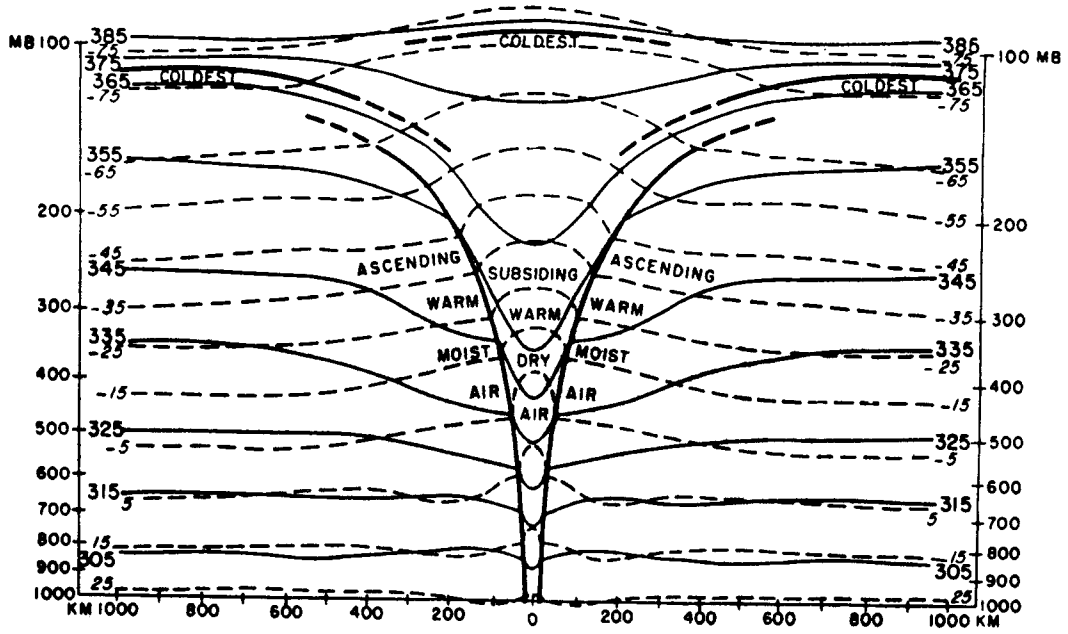

Figure 15 - Model of potential temperature (^{o}A, solid lines) and temperature (^{o}C, dashed lines) of mature hurricane in vertical cross-section. Heavy lines denote eye boundaries and tropopauses (after Palmen, 1948)

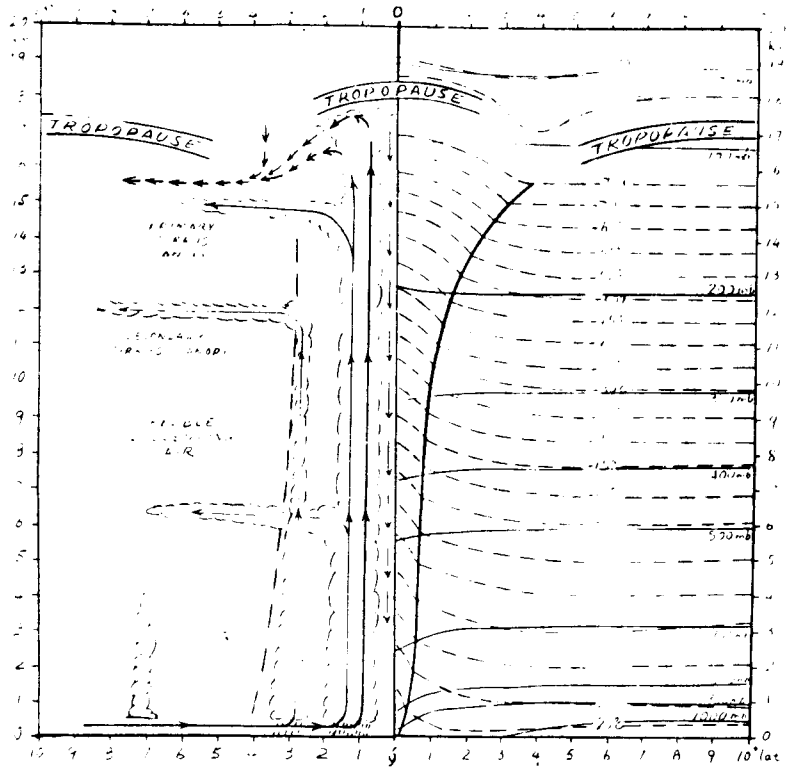

Figure 16 - Composite vertical cross-section of an "average" typhoon. Full lines depict profiles of isobaric surfaces and broken ones isotherms. The heavy full line encloses region of more marked temperature rise around the core. The thick broken line separates regions of descending and ascending motions

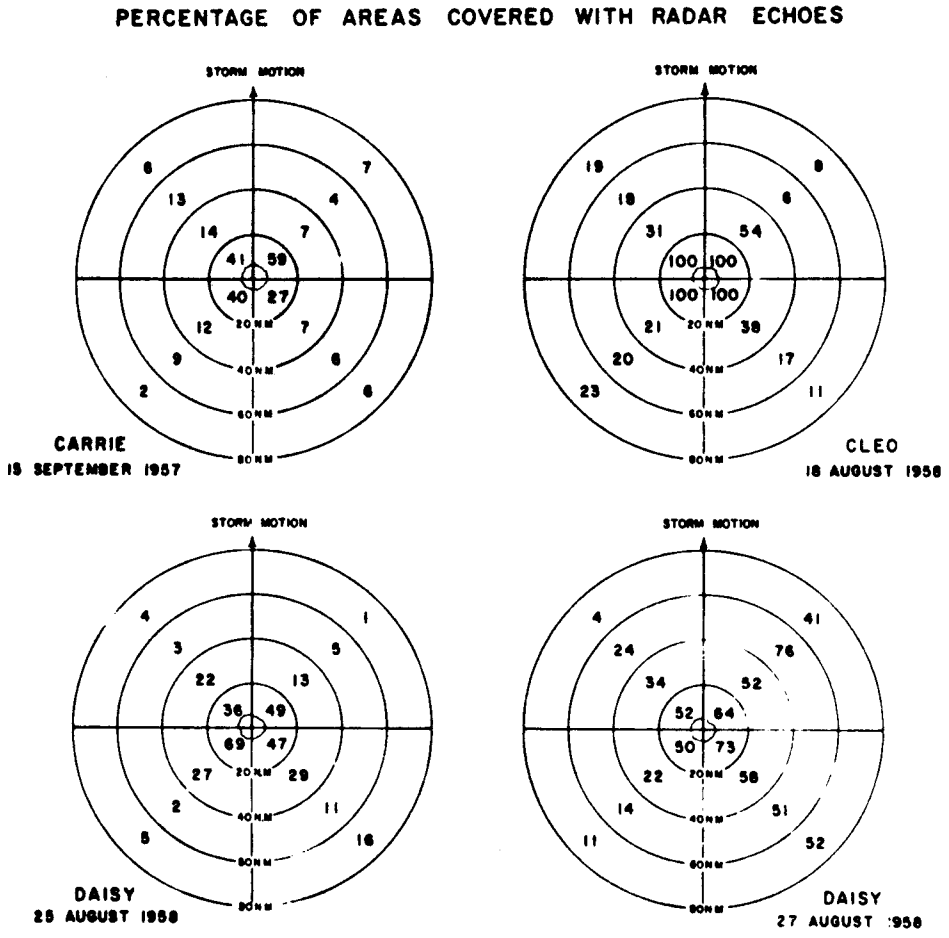

Figure 17 - Percentage of segments of hurricanes occupied by rainbands as shown by radar. The figures in the centre refer to only that portion of the area between the inner edge of the eye wall and the 20 n mi radius (after Gentry, 1964)